TECHNICAL MEMORANDUM

725

The role of shallow convection in ECMWFs Integrated Forecasting System

P. Bechtold, I. Sandu, D. Klocke,
N. Semane, M. Ahlgrimm, A. Beljaars,
R. Forbes, M. Rodwell

Research Department

July 9, 2014

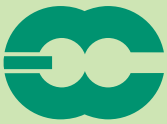

European Centre for Medium-Range Weather Forecasts
Europäisches Zentrum für mittelfristige Wettervorhersage
Centre européen pour les prévisions météorologiques à moyen terme

Series: ECMWF Technical Memoranda

A full list of ECMWF Publications can be found on our web site under:
http://www.ecmwf.int/publications/

Contact: library@ecmwf.int

European Centre for Medium-Range Weather Forecasts
Shinfield Park, Reading, RG2 9AX, England

Abstract

In the context of the European Union EUCLIPSE project the role of shallow convection was assessed in the European Centre for Medium-Range Weather Forecasts (ECMWF) Integrated Forecasting System (IFS). Three model configurations differing in the treatment of shallow convection were used to explore the impact on process tendencies, weather forecasts and climate simulations. In the summary of this work presented here, special emphasis is put on the interaction of processes and the altered balance between processes when a physical parameterization is removed, or replaced by a conceptually different approach to the treatment of shallow convection.

The activities related to boundary layer clouds that took place at ECMWF in the past few years also revealed that at present there are several inconsistencies between the parameterizations contributing to the representation of cloudy boundary layers. These inconsistencies are listed here, and a strategy towards a more consistent description of moist boundary layers is introduced. Finally, a first attempt to harmonize the computation of convective cloud base and subcloud properties across the shallow convection scheme and the turbulent diffusion scheme is described.

1 The role of shallow convection

Global Numerical Weather Prediction (NWP) models and climate models rely on parametrizations of physical processes to represent transport, mixing and phase changes that are not represented by the resolved flow, but are essential for NWP, seasonal and climate predictions. One of those parameterized processes is shallow convection. By vertically distributing moisture, heat and momentum in the boundary layer, shallow convection is an important process in the global hydrological and energy cycle (von Salzen *et al.*, 2005). Through the production of boundary-layer clouds it also strongly interacts with the radiative fluxes (Rieck *et al.*, 2012). It has been shown by Bony and Dufresne (2005) that the uncertainty in boundary-layer cloud predictions is a major contributor to the uncertainty in climate predictions. Recently, Ahlgrimm and Forbes (2012) and Nuijens *et al.* (2014) evaluated the shallow convective cloud structures in the IFS against space and/or ground-based lidar and radar observations and compared with those obtained from climate models. Their results show a fair agreement of the IFS with the observations, though a regime decomposition reveals that the IFS tends to underestimate the high cloud cover regime. For the fair weather regime, recent improvements in the cloud structure have been noted, but an underestimation of the frequency of occurence and an overestimation of the liquid water content is still present. As shown by de Rooy *et al.* (2013) the realistic fair weather cloud structure in the IFS is mainly due to an entrainment profile that closely matches LES data, while remaining errors in the liquid water content are due to the mass detrainment which turns out to be more variable and uncertain.

Figure 1 illustrates the annual mean frequency of occurrence of 'deep' convective clouds (defined as having a thickness exceeding 200 hPa and positive buoyancy) and shallow convective clouds (having a vertical extent < 200 hPa) as obtained from seasonal integrations with the IFS using the model version operational in 2012/13. The different convective types are diagnosed within the model's convection parametrization. The observed convective cloud distribution is actually tri-modal (Johnson *et al.*, 1999), but the 'deep' cloud type includes also the cumulus congestus clouds that detrain in the middle troposphere around the melting level. As shown in Figure 1a deep convective clouds are a prominent feature of the tropical belt, but also frequently occur in the middle latitude storm tracks, and the Gulf Stream and Kuroshio regions in particular. With a frequency of occurence of up to 90%, shallow convective clouds (Figure 1b) are an ubiquitous feature of the subtropical anticyclonic regions.

The climatological cloud distribution is assessed indirectly in Figure 1c by comparing the model's shortwave radiative flux at the top of the atmosphere to the shortwave flux from the Clouds and Earth's

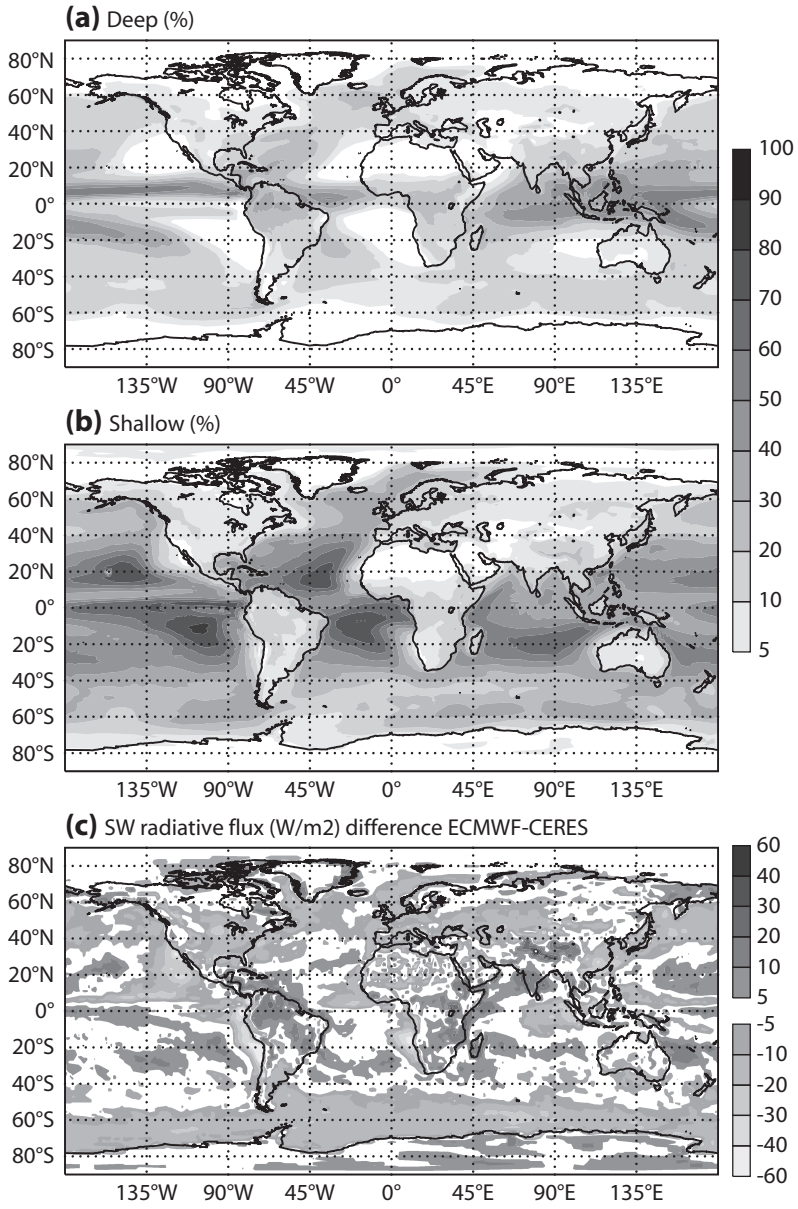

Figure 1: Annual mean frequency (%) of (a) deep and (b) shallow convective clouds as obtained from an ensemble of one-year integrations at spectral truncation T159 (125 km grid resolution) with the ECMWF model version operational in 2013. (c) Difference in climatological net shortwave radiative flux at the top of the atmosphere between the model and the Clouds and Earth's Radiant Energy Systems (CERES) Energy Balanced and Filled (EBAF) product. The sign convention is that positive values correspond to an excess in reflection (too many or optically too thick clouds), and negative values correspond to an underestimation (too few or too optically thin clouds).

Radiant Energy Systems (CERES) Energy Balanced and Filled (EBAF) product. The global mean model bias is around 10 W m^{-2}. The model errors are broadly consistent with the results discussed in Ahlgrimm and Köhler (2010): the strongest bias is in the stratocumulus areas off the West coasts of the continents, where clouds (optical thickness) are underestimated, and also in the southern hemisphere storm track where the representation of mixed phase clouds is critically important (Forbes and Ahlgrimm, 2014). The convective cloud regions are reasonably reproduced but the trade cumulus clouds are too reflective. The cloud and radiation errors strongly depend on the interactions between the physical parametrizations such as cloud and convection, the boundary-layer diffusion and the radiation as well as with the resolved dynamics. However, in tropical regions convection is the major source term for the production of clouds.

In the following we review the parametrizations that control the representation of cloudy boundary layers that are operational in the IFS and those that have been tested in the context of EUCLIPSE. We evaluate the schemes with a particular focus on:

1. moisture transport/structure and humidity errors;
2. low cloud, shortwave radiation and two-metre temperature biases;
3. low-level wind errors and momentum transport.

This is an important exercise given the above mentioned model impacts. It is also an important exercise for future developments of the IFS as shallow convection, occuring typically on characteristic scales of O(100 m), will still need to be parametrized in the years to come.

2 Boundary-layer mixing and cloud representation in the IFS

The overarching philosophy behind the IFS physical parameterizations is modularity (one scheme per process), consistency (e.g. in thermodynamical description, no double counting), order (physical processes are called in sequential order that respects the logic of forcings), and structure (schemes can be tuned with respect to some key parameters, a simplified and linear approximation of physics for data assimilation can be readily formulated). In the IFS we sequentially compute first the radiative heating rates, followed by the coupled turbulent diffusion and surface scheme, the convection scheme and finally the cloud scheme that integrates the condensate production terms from the turbulent diffusion and convection schemes. The representation of moist boundary layers depends thus on the choices made for many schemes, but here we are going to focus on the interplay of the schemes used to parameterize turbulent diffusion within convective boundary layers, shallow convection and clouds.

It is fair to say that our overall goals and philosophy have only been partially realized and we are in particular still experimenting with a more comprehensive formulation of moist boundary-layer processes. The limitations of the current operational framework used for describing these processes and possible ways to address them will be discussed in more detail in Sect. 5.

2.1 The operational framework

An Eddy Diffusivity/Mass Flux (EDMF) approach is used to represent turbulent diffusion in convective boundary layers (dry and cloudy). This scheme is based on the dry turbulent-diffusion scheme developed

by Beljaars and Viterbo (1998), that was later extended (Köhler *et al.*, 2011) to represent stratocumulus clouds via mixing of moist conserved variables and a statistical cloud scheme based on the β-function (Tompkins, 2002). Convective mixing via a mass flux contribution has also been added, though its overall contribution to the mixing is small.

The convection scheme was originally developed by Tiedtke (1989) and later thoroughly revised by Bechtold *et al.* (2004, 2008, 2014) including revisions to the subcloud parcel properties, the closure and the entrainment and detrainment profiles that strongly affect the cloud structure. Finally, the cloud scheme was originally developed by Tiedtke (1993) including prognostic equations for the cloud condensate and the cloud fraction. It has later been thoroughly revised and extended to include prognostic precipitation (Tompkins *et al.*, 2004; Forbes *et al.*, 2011).

Hence, the planetary boundary layer (PBL) includes the interacting processes of dry diffusion, cumulus mass flux, clouds and radiation. In the IFS we currently distinguish between a stable PBL, a dry convective PBL (no cloud below the level where a parcel rising from the surface stops) and a cloudy PBL. The cloudy boundary layer is further classified into either a well-mixed PBL with stratocumulus (Sc) clouds or a convective so called 'decoupled' layer with cumulus clouds. The well-mixed cloudy PBL is treated by the EDMF component of the turbulent diffusion scheme, while the non-local cloud induced convective mixing in the decoupled PBL is treated by the shallow convection parameterization. Note, however that even in the decoupled boundary-layer dry turbulent diffusion below cloud base is performed by the EDMF scheme. A stability threshold given by the estimated inversion strength (EIS) as proposed by Wood and Bretherton (2006) is used to determine if the PBL is decoupled and shallow convection is allowed. This criterion is based on earlier work by Klein and Hartmann (1993) who established an empirical relationship between lower-tropospheric thermodynamic stability and boundary layer clouds. The EIS depends upon the 700hPa and surface potential temperature difference, but weighted by the free-tropospheric temperature lapse rate that is supposed to be close to its moist adiabatic value. This makes the criterion applicable to a large spectrum of regimes including tropical and arctic boundary-layers. An EIS threshold of 7 Kelvin is used to distinguish between a decoupled boundary layer with cumulus convection and a boundary layer with Sc.

To summarize, the PBL is represented by a regime dependent switching which makes it difficult to enable smooth transitions between different regimes. There are also inconsistencies between the parcel ascent in the shallow convection scheme and that used in EDMF. In addition, EDMF uses a statistical cloud scheme that has assumptions for subgrid cloudiness that are different from the main cloud parametrization scheme. However, there are important strengths in the current operational framework. It accounts for both a quasi-dry diffusive type turbulent transport and a quasi-dry mass flux transport in EDMF, as well as a shallow moist convective ascent in the shallow convection scheme. Both schemes provide sources and sinks of humidity and cloud condensate to the main cloud scheme. Furthermore, through condensate detrainment near the inversion, the shallow convection scheme provides the main cloud source for the generation of stratocumulus. It is believed that the treatment of convection including shallow and deep convection has to be done in a unified way, in a single scheme as it is done at present, not least to provide a realistic diurnal cycle. Finally, note that the EDMF and convection schemes use separate implicit numerical solvers.

2.2 An alternative scheme: the DUAL-M

One can take a different view point and seek more consistency by integrating the shallow convection scheme in the EDMF scheme, so that EDMF contains two ascents, a dry plume stopping at cloud base and a more buoyant 'moist' parcel that reaches the cloud top. The initial near surface properties of the

plumes can be drawn from a vertical velocity distribution depending on the surface fluxes. In this framework the entire PBL mixing processes can be solved within a single implicit numerical solver. Such an approach, dubbed DUAL-M was pursued by Neggers *et al.* (2009). It also includes a statistical cloud scheme making use of diagnostic variances as obtained from the mass flux formulation (Neggers, 2009). The DUAL-M scheme has been implemented in a Single Column Model (SCM) version of the IFS as well as the full global model. The SCM and full global model evaluations (Ahlgrimm and Köhler, 2010) showed encouraging results with the DUAL-M scheme producing more realistic trade cumulus cloud structures and lower and more realistic cloud top heights than with the operational IFS framework. However, problems with the DUAL-M scheme remained, notably the underestimation of continental shallow clouds, leading to a warm bias over the continents and some lack of stabilisation in non-surface driven convection as encountered in frontal clouds. The scheme was therefore implemented with the shallow convection scheme still activated for cases when the DUAL-M does not detect shallow convective layers, in particular elevated non surface driven 'shallow' convection.

3 Impact of shallow convection in NWP and climate

To assess the importance of shallow convection, NWP and climate-type (1 year free-running) integrations have been performed with the IFS version CY38R1, corresponding to the operational version in 2012. Three different model configurations have been used: (i) the operational IFS framework for representing moist PBL (Section 2.1), (ii) the DUAL-M scheme (Section 2.2) and (iii) the operational IFS framework but with the shallow convection switched off.

The data assimilation and weather forecasts are performed at spectral resolution T511 ($\sim$40 km horizontal resolution) with 91 levels in the vertical. The 10-day forecasts are initialized every 6 hours (00, 06, 12 and 18 UTC) daily between 30 December 2011 and 2 February 2012 from an analysis which was consistently generated for each model configuration. We also compare the results to the operational HRES T1279 (16 km) system during that period. Furthermore, accumulated tendencies from physical processes are saved for the first 6 hours of each forecast to obtain a more detailed insight into the importance of the individual processes and their interactions.

The climate simulations are performed at a lower horizontal resolution with truncation T159 ($\sim$125 km), but with the same vertical resolution as used for the weather forecasts. For each model configuration a four-member ensemble is integrated over 15-months using different initial conditions and prescribed sea surface temperatures. The ensemble mean for one year after the initial 3-month spin up period is considered in this study.

3.1 Impact on NWP forecast skill

The impact of shallow convection on the NWP forecast quality is illustrated in Figure 2 for the tropical 850 hPa root mean square error (RMSE) of zonal and meridional wind speed, relative humidity and temperature. The results from the operational high-resolution T1279 (16 km) have also been added as well as confidence intervals based on the bootstrap method. The experiment with prohibited convection stands out in that it produces a significant deterioration in all variables. The results with the DUAL-M scheme are rather close to those obtained with the control operational framework (CTL), in particular in the mid-latitudes (not shown), and only produce a slight degradation in the tropics, in particular for the relative humidity. Mean temperatures below 850 hPa in the DUAL-M experiment are slightly warmer than in the CTL one with differences of about 0.1 K in the mid-latitudes and 0.2 K in the tropics. The

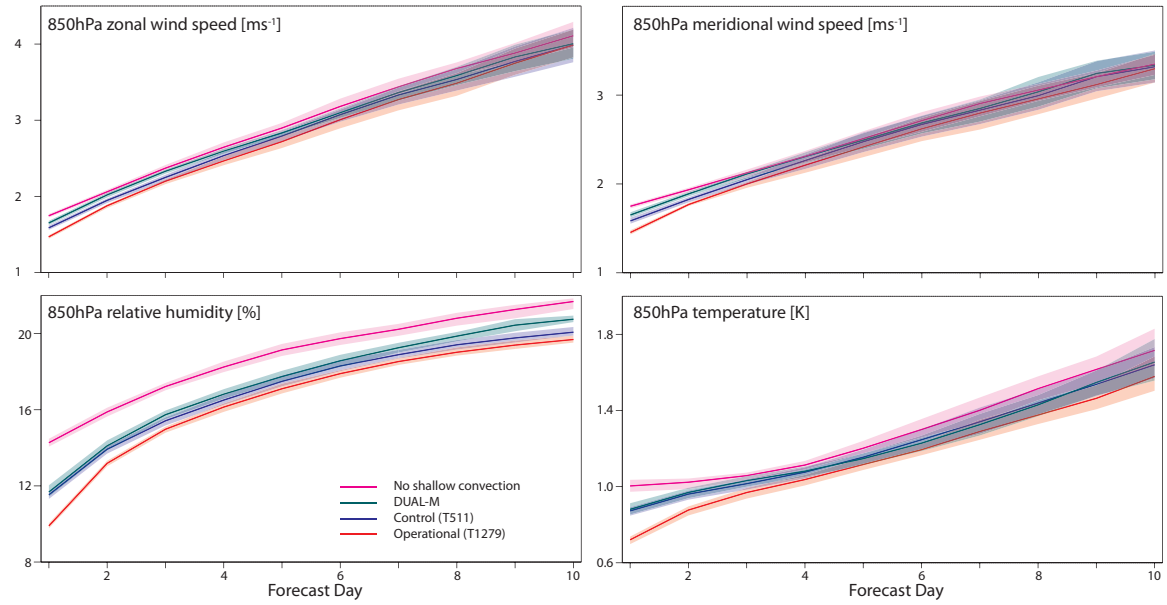

Figure 2: Evolution of the average root mean square error (RMSE) of zonal wind speed, meridional wind speed, relative humidity and temperature at 850 hPa with forecast lead time in the tropics (20°N to 20°S). Forecasts are initialized four times daily (00, 06, 12, 18 UTC) for January 2012 from their own analysis, with different model configurations for shallow convection. The shaded colors indicate the 95% confidence level according to the bootstrap method.

high-resolution forecasts are generally better than the CTL, but for longer-ranges the tropical wind forecasts barely differ from the lower-resolution control. Experience with the current ECMWF Ensemble system confirms a weak but seasonal dependent sensitivity of tropical wind scores with respect to higher horizontal resolution.

At this stage we cannot explain the rather similar results with the two shallow convection experiments and their large difference with the 'no-shallow' experiment. We do not have an experiment that allows us to quantify the contribution of the operational shallow convection scheme in the integrations with the DUAL-M, but the assumption is that the DUAL-M scheme provides most of the mixing related to surface driven shallow convection, while elevated shallow convective layers (e.g. in middle latitudes storm tracks) are dealt with by the operational convection scheme..

In Figures 3 and 4 we take a closer look at the structure and evolution of wind errors in the different experiments with respect to the CTL. All experiments are verified against their own analyses. It is clear from Figure 3 that the difference in wind errors is small between the CTL and the DUAL-M experiments, but a significant and persistent deterioration with DUAL-M is apparent in the tropical trade-wind layer. In contrast, without shallow convection (Figure 4), wind errors are largely increased both in the tropics and the mid-latitudes. During the first 12 hours this deterioration is confined to the boundary-layer, but then quickly projects onto the whole troposphere.

When repeating this analysis for temperature (Figures 5, 6 and 7) a few conclusions emerged. Differences in RMSE of temperature between DUAL-M and CTL are also small (Figure 5). However, in contrast to the wind errors for which the largest differences are seen in the lower tropical boundary-layer; the temperature differences are also seen throughout the tropical troposphere. The fact that deterioration of the temperature around 850hPa when using DUAL-M is less marked than that of the winds points to

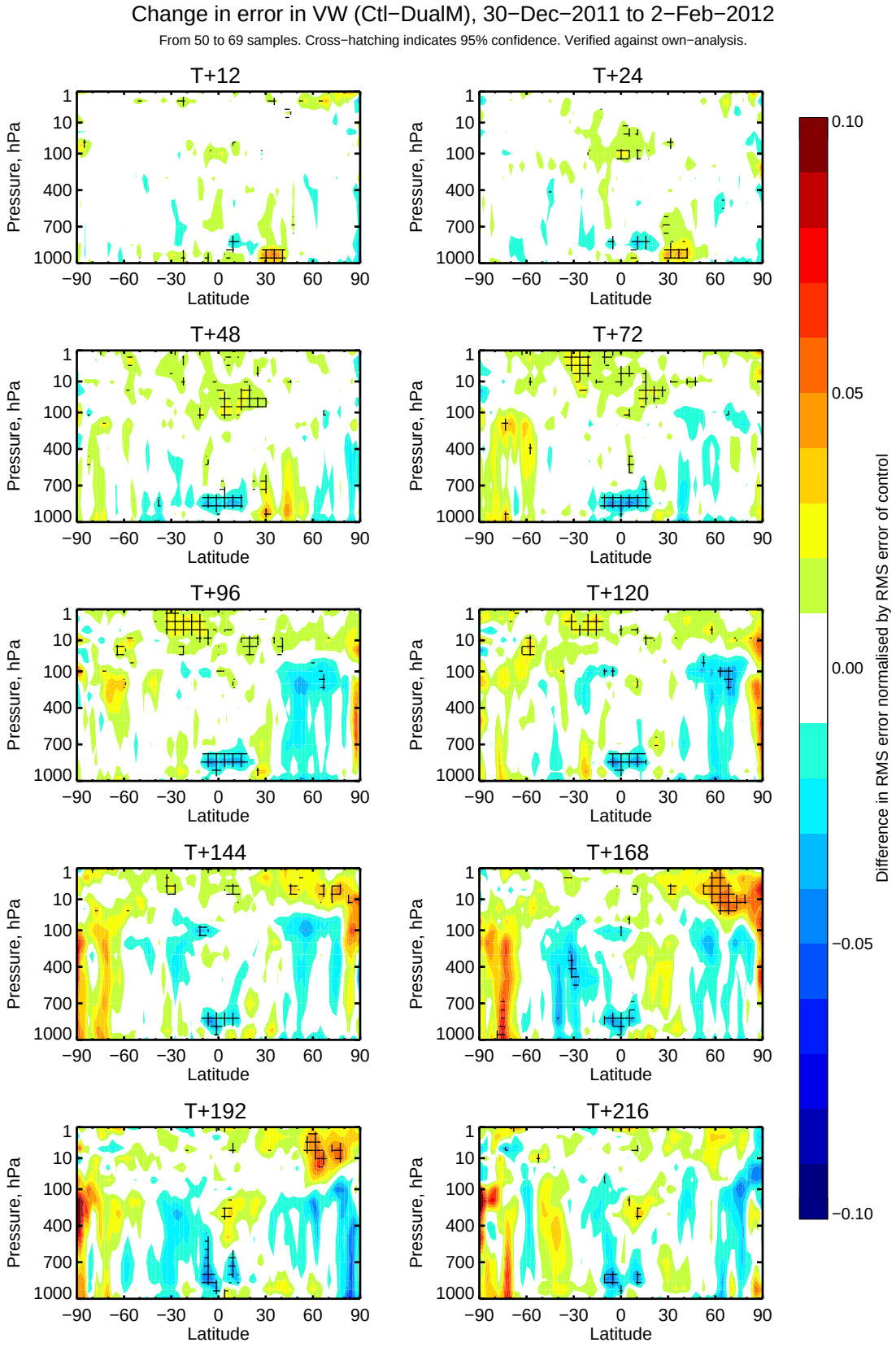

Figure 3: Zonal mean differences of wind RMSE (m/s) between the CTL and DUAL-M experiments at different forecast ranges. RMSE are against own analysis. Negative/positive values indicate that the CTL experiment is better/worse than the DUAL-M one.

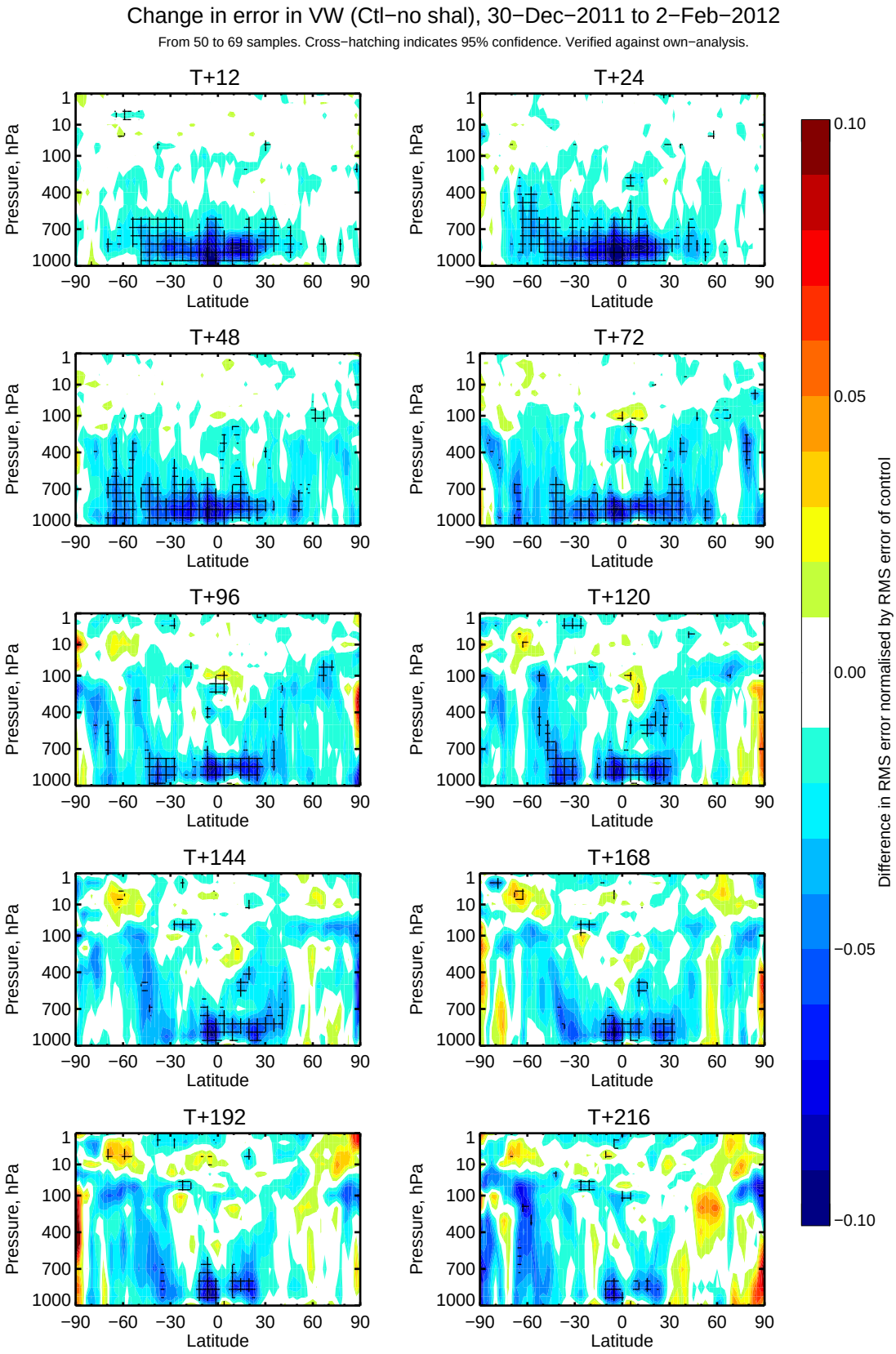

Figure 4: Same as Figure 3 but for the difference between the CTL and the no-shallow experiments

.

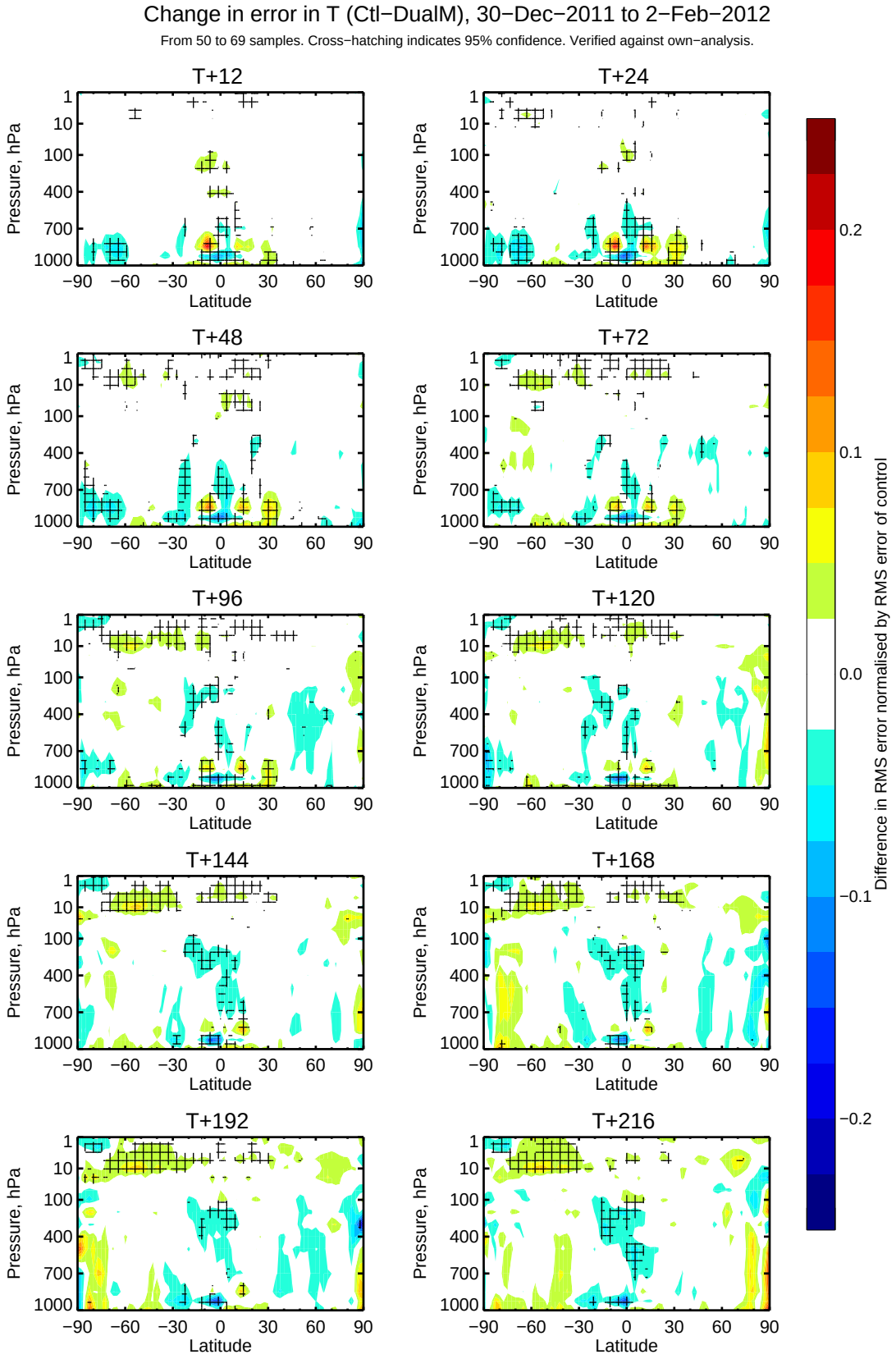

Figure 5: Zonal mean differences of rms temperature errors (K) between the control and DUAL-M at different forecast ranges. Rms errors are against own analysis.

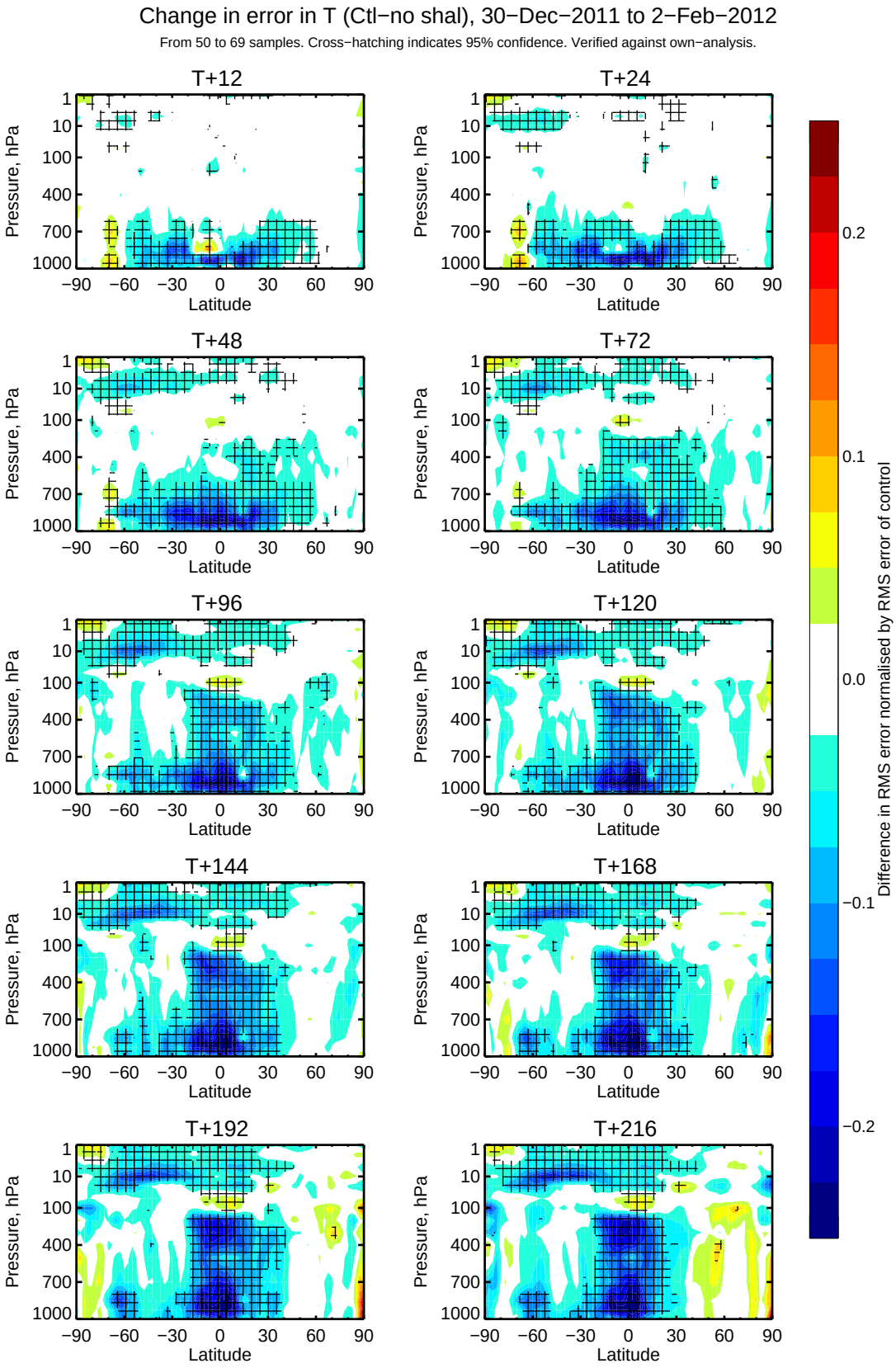

Figure 6: Sames as Figure 5 but for the difference between the control and no-shallow

.

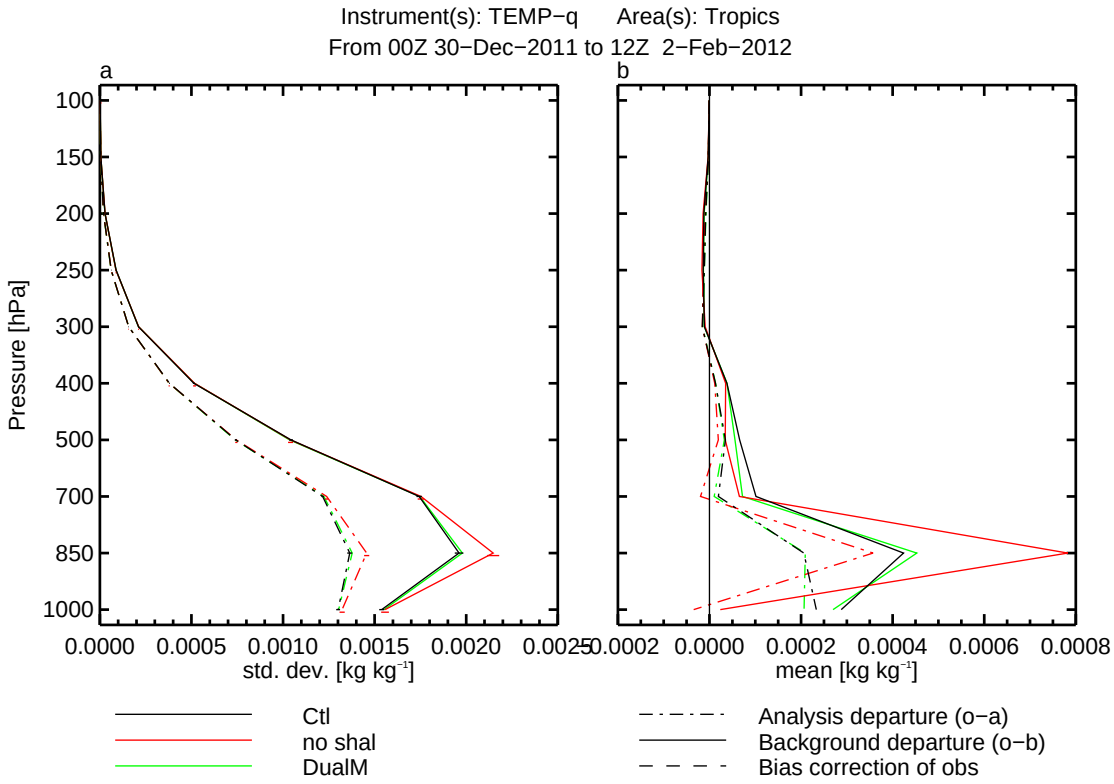

Figure 7: First guess specific humidity departures (g kg^{-1}) against tropical radiosondes for control, DUAL-M and no-shallow experiments.

some lack of momentum transport in DUAL-M. As expected, the differences in the rmse of temperature between CTL and the no-shallow experiment (Figure 6) are large in the lower troposphere, notably in the tropics and southern hemisphere storm tracks, and persistent throughout the forecast range. Finally, the large change in the boundary-layer vertical transport in the no-shallow experiment is also apparent from the short-range humidity errors plotted in Figure 7 as the first-guess departures from the tropical radiosondes. The mean departures (obs - model) attain a value of roughly +1 g kg^{-1} (model too dry) at 850 hPa, but little change at 1000 hPa.

Increased model biases and error growth are most likely caused by either imbalances between individual model processes or a lack of physical realism. How the model processes and their balance adjust to changes in the shallow convection is discussed next.

3.2 Individual processes and compensating effects

In order to quantify the contributions of the individual processes and their overall balancing or compensating effect, zonal mean forecast temperature tendencies (accumulated over the first 6 hours and then summed over the 4 forecasts per day; see Rodwell and Palmer (2007) for a discussion of this approach) during the first 24h of the forecasts are plotted in Figure 8 for the CTL experiment together with the corresponding analysis increments for temperature and wind. Heating by convection dominates in the tropical troposphere but also in the wintertime mid-latitude storm track regions, while in the subcloud layer (lower boundary-layer) convection has a cooling effect due to the evaporation of rain. Diffusive

heat transport dominates in the boundary-layer where it is mainly compensated by dynamical cooling. In the tropical free troposphere a broad equilibrium is established between the convective heating and the cooling resulting from radiation, dynamics (vertical motion) and the cloud scheme. The net cooling effect of the cloud scheme in this region is due to the evaporation of precipitation and condensate detrained by the convection scheme, which dominates over the warming effect associated with latent heat release during condensation (condensational heating dominates in regions where the convection is less present, i.e. upper troposphere in the mid-latitudes). The radiative tendency (cooling) is rather uniform globally, but with a peak cooling rate near 800 hPa in the storm tracks. In the troposphere, the resulting temperature increment (analysis - model evolution) is largest in the tropics and the polar regions, where the forecasts tend to have a dipole cooling/warming effect of O(0.2 K). The tropical meridional circulation increments (not shown) indicate that the forecasts tend to decrease the intensity of the Hadley circulation.

The differences in the individual temperature tendencies between the no-shallow convection experiment and the CTL are depicted in Figure 9. The reduction in the convective heating rates clearly displays the regions where 'shallow' convective heating operates in the IFS, ie. the 800-900 hPa layer, but also, albeit with a weaker amplitude, in the free troposphere as elevated shallow convection. The reduction in convective heating is mainly compensated by additional heating through vertical diffusive transport and condensational heating in the cloud scheme. As explained above the cloud scheme influences the temperature evolution through two processes: the condensational heating and the evaporative cooling. When the shallow convection is turned off, the evaporative cooling decreases because there is less precipitation and less condensate detrained from the convection, so the cloud scheme has an overall warming effect compared to the CTL experiment. Due to the increased cloud amount, the low-level radiative cooling is strongly increased. The changes in the dynamics are much smaller, partly because the zonal-mean resolved circulation is better constrained in the analyses by the observations (which are common to both sets of analyses) - the increment change takes up some of the warming at 850hPa instead of the dynamics. Differences in the circulation and the dynamical tendencies will, however, grow into the medium-range forecast. From the mean difference in analyses, notice that the inversion at the top of the PBL is stronger in the absence of parameterized shallow convection.

The tendency differences between DUAL-M and CTL are depicted in Figure 10. One observes a similar reduction in convective tendencies in the PBL as seen in Figure 9, but there is no change in the free troposphere (recall that in the DUAL-M implementation shallow elevated convection is represented by the control shallow convection scheme). A similar compensatory warming as in the no-shallow run is apparent in the cloud tendencies. The difference in diffusive heating with respect to the CTL shows a dipole structure, suggesting than the vertical transport is less intense with DUAL-M than in the CTL configuration. Differences in dynamical and radiative tendencies are small, with a net heating effect due to less PBL clouds. Overall, the results with the DUAL-M are somewhat in between those with the CTL and the no-shallow experiment. The effect on the increments is mainly a cooling increment change, with a warming increment change in the tropical uppertroposphere. By comparison with Fig. 5, it can be seen that both these aspects are desirable in that they result in smaller mean increments in the tropics.

As we have seen complex compensatory effects and interactions between parametrizations operate that can make it difficult to identify root causes for model systematic errors, and even more so to correct these errors. This is especially true for the boundary-layer where changes in turbulent mixing near the boundary-layer top strongly interact with clouds and radiation (Bretherton and Wyant, 1997; Köhler *et al.*, 2011; Sandu *et al.*, 2012) and where changes in moisture and stability project onto the deep tropical modes (Bretherton *et al.*, 2004; Raymond and Fuchs, 2009; Bechtold *et al.*, 2008; Hirons *et al.*, 2013, 2012). In the following, we evaluate the experiments concerning their climate impact and put the

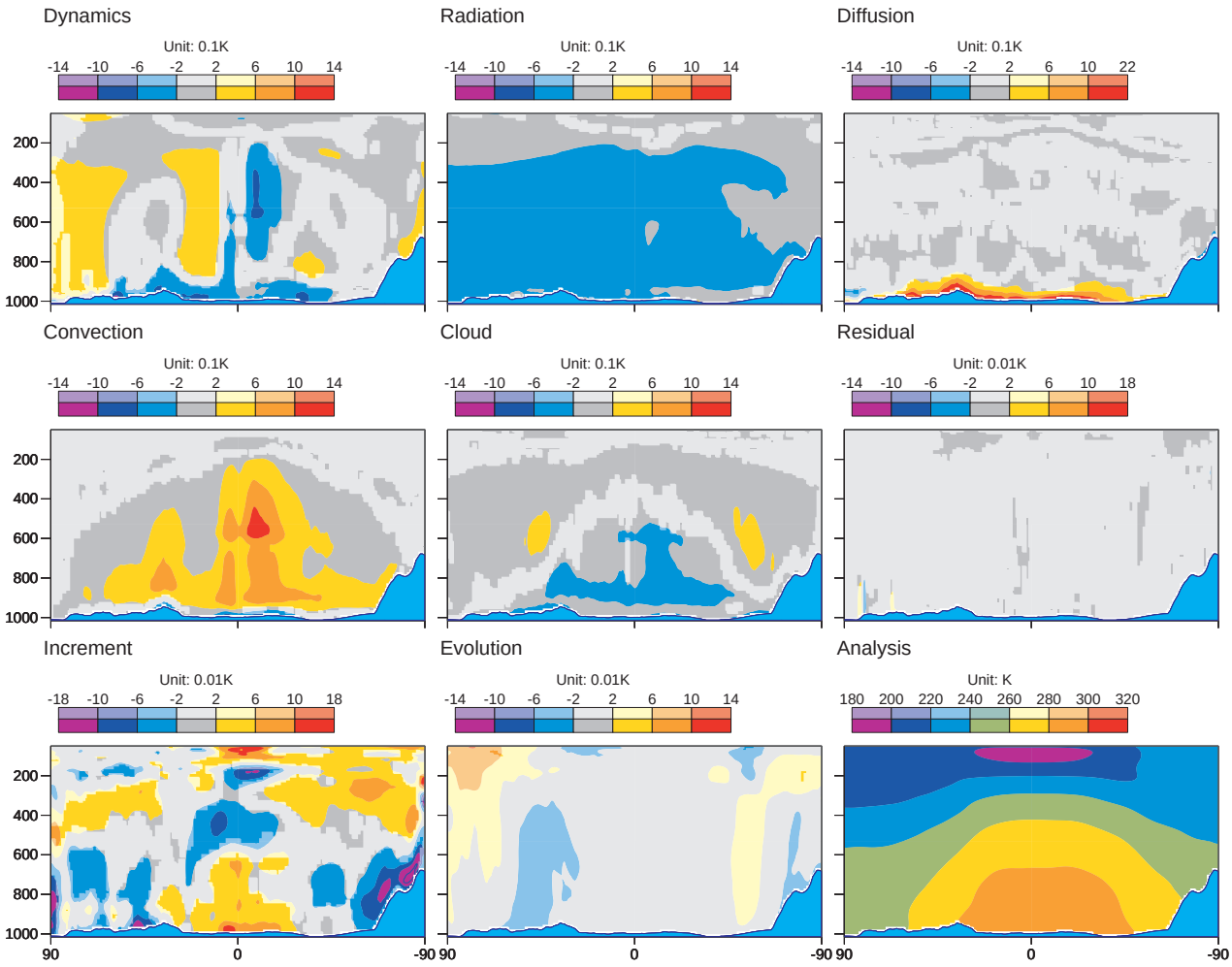

Figure 8: Zonal and monthly mean temperature tendencies (K/6 h, averaged over the four daily 6-hourly forecasts) from the dynamics and the individual physical process during January 2012, as well as monthly mean analysis increments, the mean temperature from the analysis, the evolution of the analysis and the residual. The evolution of the analysis and the residual are expected to be small. Deep colours denote 5% significance.

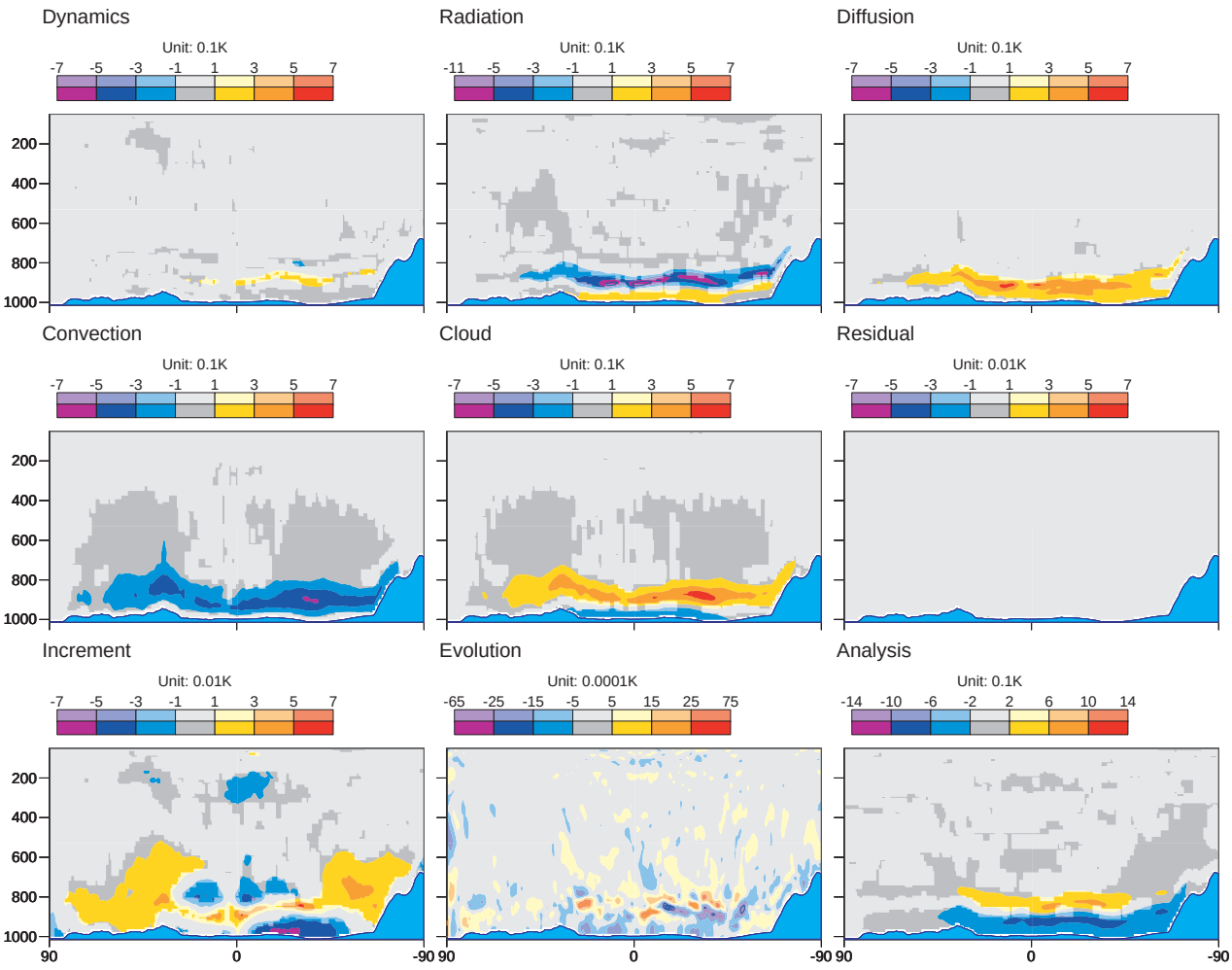

Figure 9: Same as Figure 8, but for differences in the individual tendencies, increments and analysis between the no-shallow experiment and CTL.

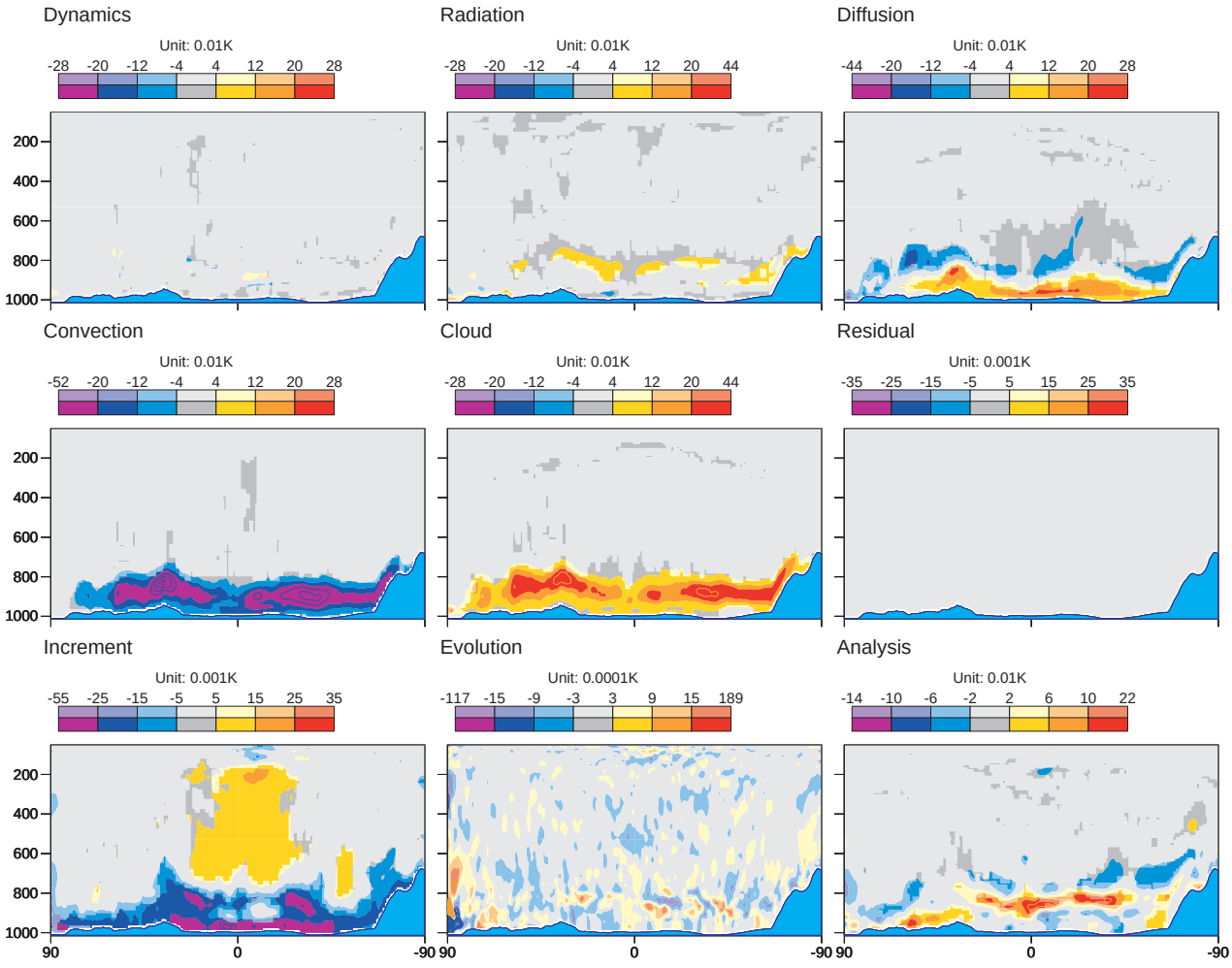

Figure 10: Same as Figure 9 but for differences between the DUAL-M and CTL. (Note different contour scales).

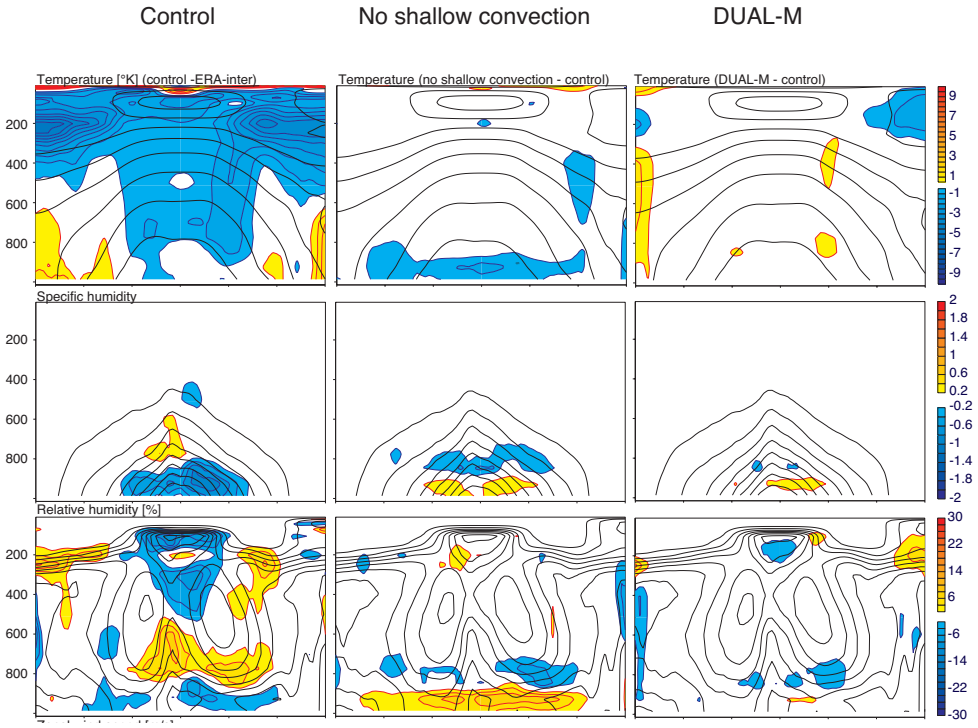

Figure 11: Mean climate error in temperature, specific humidity, relative humidity and zonal wind speed of the control model relative to ERA-interim (left column), a climate simulation without shallow convection relative to the control simulation (middle column) and a climate simulation with DUAL-M relative to the control simulation (right column).

long term impact in perspective to the short-range differences discussed so far.

3.3 Climate impact

Climate simulations reveal large differences between the simulations with different boundary layer treatment as demonstrated in Figure 11 for temperature, specific and relative humidity. The control model is shown relative to the ERA-Interim. In order to highlight the impact of model changes, the simulations without shallow convection and DUAL-M are shown relative to the control.

Without shallow convection (centre column in Figure 11) a zonal mean cooling is established. Referring to Figure 9 this is mainly due to increased cloud radiative cooling associated with the increase in cloudiness that results from the reduced vertical transport of heat and moisture. Indeed, the lack of moisture transport leads to an accumulation of specific humidity in the PBL while the trade-wind layer and lower free troposphere become drier. The combination of cooling and moistening increases the relative humidity close to 100% near the top of the subcloud layer over large regions in the tropics and sub-tropics and the cloudiness increasing significantly. The simulations with DUAL-M (right column in Figure 11) show a similar dipole pattern for the specific and relative humidity fields with respect to the control, though with much reduced amplitude. However, the zonal mean temperature structure of the DUAL-M is close to that of the control, with the DUAL-M producing slightly warmer temperatures near the top of the tropical PBL.

The effect of shallow convective momentum transport with deceleration of the flow in the trade wind

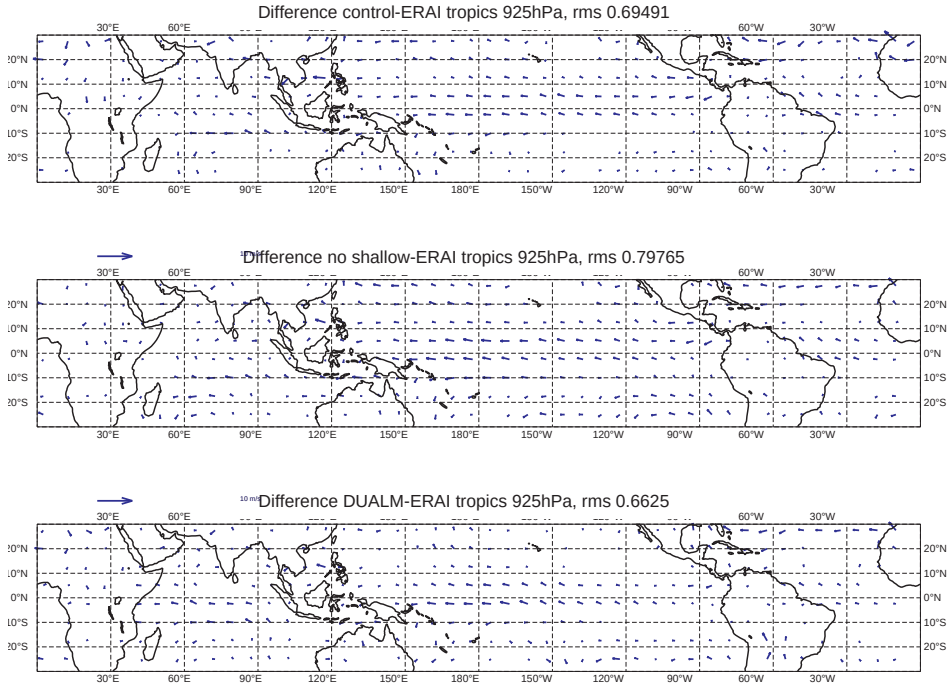

Figure 12: Difference in annual mean 925 hPa wind between the CTL, no-shallow, DUAL-M climate simulations and ERA-Interim.

layer and an acceleration of the near surface winds is also readily apparent from the 925 hPa maps in Figure 12. Without shallow convection the easterly flow in the central and western Pacific region is largely overestimated, increasing the already existing easterly wind bias in the model. However, and this is consistent with the NWP results in Figure 2, the difference in low-level winds between DUAL-M and the control is small.

The effect on low cloud cover, two-metre temperature and boundary-layer height is illustrated in Figure 13. Without shallow convection, low cloud cover is increased globally by 23 %, with even larger increases in the subtropical anticyclonic regions (compare also to 1b). This is accompanied by a substantial low-level cooling over land (sea surface temperatures are prescribed) and a global increase in boundary-layer height of more than 100 m, with again even larger differences in the subtropical anticyclonic regions. In contrast, with the DUAL-M low cloud cover is globally decreased by 7%, with particularly strong decreases over land, in the southern hemispheric storm tracks and the tropical belt, though low cloud cover is increased in the stratocumulus regions. The latter regions show also an increase in boundary-layer height by roughly 100 m. As a consequence of the reduction in cloud cover, land temperatures increase by 1-2 K in the annual mean. The low cloud changes induced by DUAL-M reduce model biases over the tropical oceans (see also 1c), but increase them over land. This is consistent with experiences from earlier versions of the DUAL-M in the IFS. Overall, our results on the climate impact of shallow convection are consistent with those presented by von Salzen *et al.* (2005) and Park and Bretherton (2009) who also noted a substantial increase in vertical transport, reduced cloud amount and improved radiative forcing when a shallow convection scheme is employed. However, our results partially differ from the authors in that we found (not shown) also a notable reduction in tropical rainfall by shallow convection with respect to the no-shallow experiment through a change in lower-tropospheric stability.

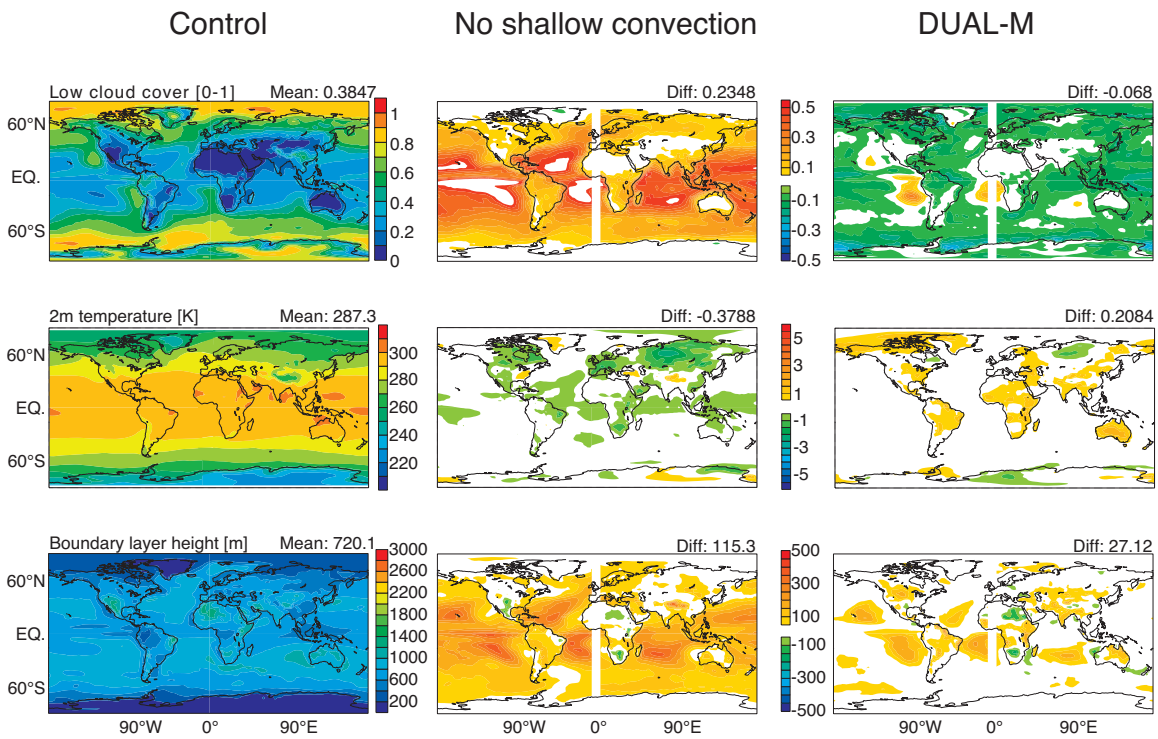

Figure 13: Left column: Mean low cloud cover ($p > 0.8p_{sfc}$), 2 metre temperature and boundary layer height in the CTL climate simulation. Middle and right columns: differences in these three parameters between the climate simulation without shallow convection and the CTL, and the climate simulation with DUAL-M and the CTL, respectively.

4 Toward a more consistent description of moist PBL

Our recent work focusing on the representation of boundary layer clouds with the ECMWF IFS (Sect. 3, Bauer *et al.* (2013), Ahlgrimm and Forbes (2014)) revealed that at present there are inconsistencies between the relevant parametrization schemes (EDMF, shallow convection and cloud schemes). We believe that further progress in the representation of boundary layer clouds and in the overall performance of the IFS can be made by simplifications and adaptations of the operational IFS framework, that would aim to increase the consistency between the above mentioned schemes. In particular, we believe that the 'dual mass flux' framework is promising and that it can be realized within the current framework and without the inconsistency of implying an additional statistical cloud scheme. Our strategy is to maintain the dry turbulent diffusion scheme and the dry mass flux transport (dry plume) while the shallow convection scheme would represent the moist convective transport (moist plume) including for Sc. This would require non-negligible modifications to both EDMF and the shallow convection schemes. These modifications are the subject of ongoing work and will be described in a future report.

For the time being, we limit ourselves here to reviewing the shortcomings of our current framework for representing moist boundary layers (points a to d below), and the first steps taken to address them:

(a) One aspect that needs particular attention is the uplift of the parcel used to determine the boundary layer top. Moist parcels rising from the surface are used to determine the boundary layer top in the EDMF scheme and the level of zero buoyancy of the updraft in the shallow convection scheme. In theory these two levels should be identical, but they are not. It was shown that part of the difference comes from the formulation of the entrainment rate in the rising parcels. An intermediate solution was found to improve the agreement between these two parcels, but this is not entirely satisfactory (Bauer *et al.*, 2013). In a recent EUCLIPSE funded activity, the two parcels have been more thoroughly compared in order to understand the remaining differences. The conclusions of this work are reported in the following subsection.

(b) Currently the stratocumulus are, at least partially, treated within the EDMF framework, while the shallow cumulus clouds are treated by the shallow convection and the cloud scheme. The criterion for deciding whether the PBL cloud is a stratocumulus or a shallow cumulus is a threshold value of the EIS (as explained in Sect. 2.1). This is not satisfactory, mainly because different regions are characterized by different inversions strengths (for example the EIS has much larger values in the South East Pacific than in the North East Alantic subtropical regions where stratocumulus clouds regularly occur), but also because it does not ensure a smooth transition between boundary layer cloud regimes. The planned changes to the EDMF and shallow convection schemes will seek to make such transitions smoother, avoiding the use of fixed thresholds.

(c) In the EDMF framework a parameterization is applied to mimic the subgrid mixing in the stratocumulus clouds due to radiative cooling at cloud top and to represent the cloud top entrainment. One of the big shortcomings of this approach is that the EDMF scheme is active only when the boundary layer is convective. This means that the subgrid mixing and the explicit cloud top entrainment are not included during nighttime over land or winter cases when the stratocumulus cloud is above a stable layer. We are currently attempting to also apply the radiatively driven subgrid mixing in these cases. Inspiration is provided by the works of Bretherton and Park (2009) and Lock, 2004 and Lock, personal communication.

(d) The EDMF uses a set of moist conserved variables. When the PBL type is determined to be 'stratocumulus' (i.e. the parcel ascent detects a cloud base and the EIS criterion is satisfied), the EDMF scheme determines cloud fraction in a statistical manner, assuming a cloud condensate distribution in the shape of a β-function (Tompkins, 2002) and diagnoses tendencies for the prognostic cloud variables (liquid

and ice condensate and cloud fraction). The EDMF assumptions are different to the subgrid variability assumptions in the main cloud parametrization (Tiedtke, 1993) and inconsistencies can arise.

4.1 Inconsistencies between the EDMF and shallow convection parcel ascents

In the following we describe the reasons for the current inconsistencies between the 'parcels' used in the EDMF and shallow convection schemes (CONV hereafter). Parcels of air, moister and warmer than the environment, rising from the surface are used in the two schemes as a proxy for the convective updrafts. The level where they become neutrally buoyant with respect to their environment (the zero-buoyancy level) indicates the boundary layer top (clear or cloudy) in EDMF, and the cloud top in the shallow convection scheme. As explained in point (a) above, the EDMF and CONV parcels often do not find the same zero-buoyancy level, despite the recent attempts to diminish the discrepancies between their formulations in IFS Cy38R2 (Bauer *et al.*, 2013).

To illustrate the discrepancies between the two parcels and the attempt to reduce them, we use Single Column Model (SCM) simulations of two idealized cases that have been used for model intercomparisons in the GEWEX Cloud System Study (GCSS) framework. One case is a stratocumulus to cumulus transition, based on Sandu *et al.* (2010); Sandu and Stevens (2011), while the second case is a cumulus case based on the BOMEX dataset (Nitta and Esbensen, 1974). The SCM is based on IFS Cy38r2.

4.1.1 Why does consistency of parcel ascent algorithm matter?

Figs. 14 and 15 illustrate the time evolution of the zero-buoyancy level (top panels) for the EDMF (black) and the CONV (full blue) parcels for the two idealized cases, as well as the boundary layer and the convective types throughout the SCM runs. Although the SCM predicts cloud most of the time in the two cases (Figs. 16 and 17), the EDMF parcel indicates a cloudy boundary layer only in the first 24 hours of the transition run, when it detects a stratocumulus (PBL type 2, Fig. 14), and for a brief period in the BOMEX case when it detects a decoupled PBL with shallow cumulus (PBL type 3, Fig. 15). For the rest of the two simulations, the EDMF parcel indicates a dry PBL, which means the parcel stops before reaching the cloud base, while the CONV parcel indicates that either shallow or mid-level convection is present (PBL type 1 versus CONV type 2 or 3, Figs. 14 and 15). In these cases, the EDMF parcel stops sometimes lower than the CONV one (for example, in the second part of the transition case, when the black line is lower than the blue line). However, at other times, although it reaches the same level (some parts of the BOMEX run) it still indicates that there is no cloud below that level, while the CONV parcel finds a cloud base (PBL type 1 vs CONV type 2 or 3).

This behaviour which is also frequently encountered when diagnosing the same quantities from 3D simulations (not shown) is unsatisfactory for several reasons:

- in undetected stratocumulus cases (PBL type 1 instead of 3 - see Fig. 14 for PBL and CONV types definition), the supplementary mixing associated with cloud top radiative cooling and the cloud top entrainment parametrization (see point c above) is not applied;
- in undetected decoupled cases (PBL type 1 instead of 3) an entrainment rate of 20% is applied at the PBL top instead of no entrainment rate (which is the current choice for PBL type 3, when the clouds are treated by the shallow convection scheme and no entrainment at the top of the PBL is applied in EDMF);

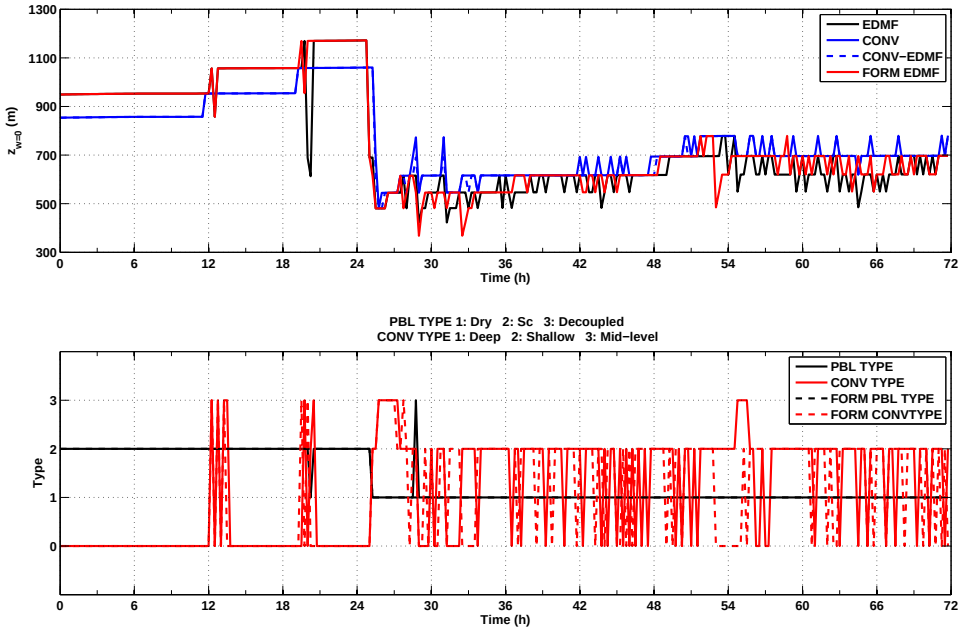

Figure 14: Top: Time evolution of the zero-buoyancy level in the transition case run, as detected by the EDMF parcel (black), CONV parcel (blue), CONV parcel called from EDMF (dashed blue), a modified EDMF parcel so that it has the same formulation as the CONV parcel (red). More details about the last two runs are given in Sect. 4.1.2. Bottom: Time evolution of the PBL and CONV types in the control runs (full), and the run where the formulation of the EDMF parcel is changed so that it matches that of the CONV parcel. The PBL and CONV types are defined in the title.

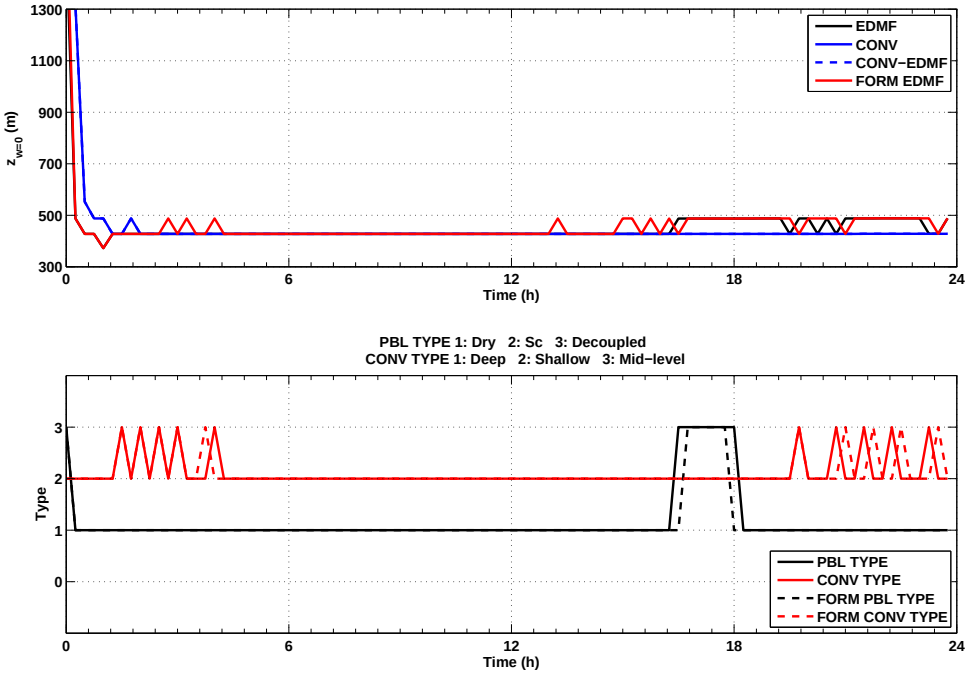

Figure 15: Same as 14 but for the BOMEX case.

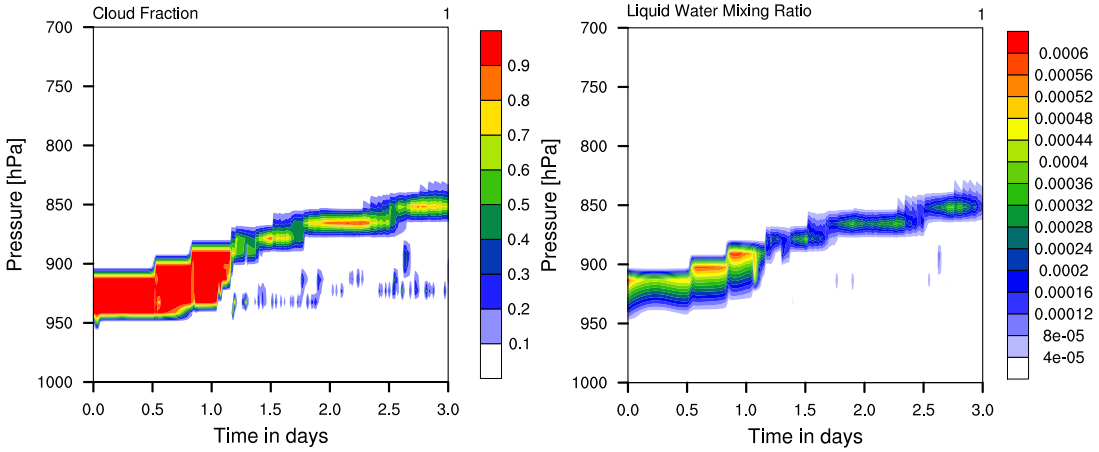

Figure 16: Time evolution of the cloud fraction (left) and liquid water mixing ratio (kg/kg) (right) in the control simulation of the transition case.

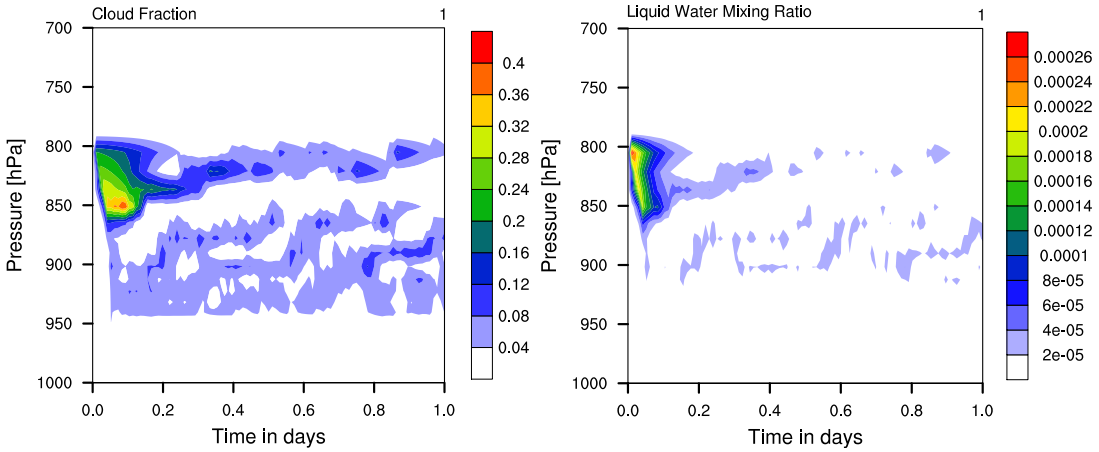

Figure 17: Same as 16 but for the BOMEX case.

- in both cases, the mixed layer parameterization for turbulent mixing it is not applied as it should be up to the cloud top (in Sc cases) or cloud base (in decoupled case), but is only applied up to the level zero-bouyancy found by the EDMF parcel.

4.1.2 Possible reasons for disagreement of the zero buoyancy level

There are a number of reasons for the lack of agreement between the EDMF and the CONV parcel ascent and diagnosis of the zero buoyancy level and two candidates are described here.

CONV is called after the turbulent diffusion scheme and a pre-call to the cloud scheme. So it is well possible that it sees slightly different profiles of temperature and humidity than EDMF, and therefore predicts a different zero-buoyancy level. This hyphothesis can be easily tested by doing the following experiment. A 'fake' call to CONV is made at the beginning of EDMF, with the only purpose of diagnosing the zero-bouyancy level (all the other outputs of CONV are not used in EDMF). It appears that

even if CONV would be called at the same time as EDMF, and would 'see' the same profiles, it would still predict a different zero-buoyancy level from the one of the EDMF parcel (dashed blue line in Figs. 14 and 15). Indeed the zero-buoyancy level predicted by the CONV call within EDMF is very close (or identical for BOMEX) to that predicted in the real call to CONV (dashed versus full blue line in Figs. 14 and 15).

The second obvious reason for the two parcels to give different results are differences in their formulation. The two parcels are based on a single bulk plume model, as described in Section 3.3.1 and Section 6.4, respectively, of part IV of IFS documentation Cy38r1. The formulations of the two parcels are different in a few respects:

- the assumption for the temperature and humidity excess, and the friction velocity used in their computation;
- the initialization of the updraft velocity;
- the numerical solution for solving the updraft equation;
- the level where the entrainment is applied.

To assess the impact of these differences the EDMF parcel is changed so that it uses exactly the same formulation as the CONV parcel. However, this brings little improvement if any to the EDMF parcel. Even if the EDMF parcel rises a bit higher in some cases, i.e. towards the end of the transition case, it still does not detect a cloud layer more frequently than in the control version (Figs. 14 and 15).

The remaining differences between the two parcels are more fundamental. For example, EDMF works in conserved variables space, while CONV does not; CONV uses sligthly modified profiles of temperature and humidity due to the different way of defining the half levels; the algorithm for defining the cloud base is different. These differences cannot be addressed without entirely recoding the EDMF parcel algorithm. Another solution, which makes more sense given our current effort to make a more seamless interaction between the two schemes, is to use the CONV parcel in both schemes. This is currently the subject of a larger project of rewriting and simplifying the convective processes in the boundary-layer scheme and will be described in a future report.

5 Conclusions

We have quantified the impact of shallow convection on the IFS forecasts in terms of analysis increments, medium-range forecast errors and climate wind, temperature and cloud/radiation biases. It became clear that without shallow convection, the model is not able to compensate for the lack of heat and momentum transport, leading to an overestimation of low-level moisture and boundary-layer clouds and to an overestimation of the winds in the trade-wind layer.

We have also described our plans for a more consistent treatment of dry and moist convective transport and mixing across the boundary-layer scheme and the convection scheme. These include a unified dry and moist parcel ascent, a consistent treatment of mixing in the cloud-layer and a consistent coupling to the cloud scheme of the IFS. It is hoped that these developments will not only provide a simpler, easier to maintain and more linear code, but will also address known boundary-layer cloud problems (underestimation of subtropical stratocumulus, overestimation of tropical cumulus and the representation of Arctic mixed-phase clouds), and improve the representation of the low-level flow in the Asian summer monsoon.

References

Ahlgrimm, M., and R. Forbes, 2012: The impact of low clouds on surface shortwave radiation in the ECMWF model. *Mon. Wea. Rev,* **140**, 3783–3794.

Ahlgrimm, M., and R. Forbes, 2014: Improving the representation of low clouds and drizzle in the ECMWF model based on ARM observations from the Azores. *Mon. Wea. Rev,* **142**, 668–685.

Ahlgrimm, M., and M. Köhler, 2010: Evaluation of Trade Cumulus in the ECMWF Model with Observations from CALIPSO. *Mon. Wea. Rev,* **138**, 3071–3083.

Bauer, P., A. Beljaars, M. Ahlgrimm, P. Bechtold, J. Bidlot, M. Bonavita, A. Bozzo, R. Forbes, E. Holm, M. Leutbecher, P. Lopez, L. Magnusson, F. Prates, M. Rodwell, I. Sandu, A. Untch, and F. Vitart, 2013: Model Cycle 38r2: Components and Performance.

Bechtold, P., M. Köhler, T. Jung, F. Doblas-Reyes, M. Leutbecher, M. Rodwell, F. Vitart, and G. Balsamo, 2004: The simulation of the diurnal cycle of convective precipitation over land in global models. *Quart. J. Roy. Met. Soc.*, **130**, 3119–3137.

Bechtold, P., M. Köhler, T. Jung, F. Doblas-Reyes, M. Leutbecher, M. Rodwell, F. Vitart, and G. Balsamo, 2008: Advances in simulating atmospheric variability with the ECMWF model: From synoptic to decadal time-scales. *Quart. J. Roy. Met. Soc.*, **134**, 1337–1351.

Bechtold, P., N. Semane, P. Lopez, J. Chaboureau, A. Beljaars, and N. Bormann, 2014: Representing Equilibrium and Nonequilibrium Convection in Large-Scale Models. *J. Atmos. Sci.*, **71**, 734–753.

Beljaars, A. C. M., and P. Viterbo, 1998: The role of the boundary layer in a numerical weather prediction model. In A. A. M. Holtslag, and P. G. Duynkerke (Eds.), *Clear and Cloudy Boundary Layers*. North Holland Publishers.

Bony, S., and J. L. Dufresne, 2005: Marine boundary layer clouds at the heart of tropical cloud feedback uncertainties in climate models. *Geophys. Res. Let.*, **32**, L20806.

Bretherton, C., and M. C. Wyant, 1997: Moisture transport, lower-tropospheric stability, and decoupling of cloud-topped boundary layers. *J. Atmos. Sci.*, **54**, 148–167.

Bretherton, C. S., M. E. Peters, and L. E. Back, 2004: Relationships bewteen water vapor path and precipitation over the tropical oceans. *J. Climate,* **17**, 1517–1528.

de Rooy, W., P. Bechtold, K. Fröhlich, C. Hohenegger, H. Jonker, S. Mironov, J. Teixeira, and J.-I. Yano, 2013: Entrainment and detrainment in cumulus convection: An overview. *Quart. J. Roy. Met. Soc.*, **139**, 1–19.

Forbes, R., and M. Ahlgrimm, 2014: On the representation of high-latitude boundary layer mixed-phase cloud in the ECMWF global model. *Mon. Wea. Rev,* **142**, In press.

Forbes, R., A. M. Tompkins, and A. Untch, 2011: A new prognostic bulk microphysics scheme for the IFS. ECMWF Technical Memorandum No. 649, 30 pages, available from ECMWF, Reading, UK.

Hirons, L., P. Inness, F. Vitart, and P. Bechtold, 2012: Understanding advances in the simulation of intraseasonal variability in the ecmwf model. part ii: The application of process based diagnostics. *Quart. J. Roy. Met. Soc.*, **139**, 1427–1444.

Hirons, L., P. Inness, F. Vitart, and P. Bechtold, 2013: Understanding advances in the simulation of intraseasonal variability in the ECMWF model. Part I: The representation of the MJO. *Quart. J. Roy. Met. Soc.*, **139**, 1417–1426.

Johnson, R. H., T. M. Rickenbach, S. A. Rutledge, P. E. Ciesielski, and W. H. Schubert, 1999: Trimodal characteristics of tropical convection. *J. Climate*, **12**, 2397–2418.

Klein, S., and D. Hartmann, 1993: The seasonal cycle of low stratiform clouds. *J. Climate*, **6**(8), 1587–1606.

Köhler, M., M. Ahlgrimm, and A. Beljaars, 2011: Unified treatment of dry convective and stratocumulus-topped boundary layers in the ECMWF model. *Quart. J. Roy. Met. Soc.*, **137**(654), 43–57.

Neggers, R., 2009: A Dual Mass Flux Framework for Boundary Layer Convection. Part II: Clouds. *J. Atmos. Sci.*, **66**, 1488–1506.

Neggers, R., M. Köhler, and A. Beljaars, 2009: A Dual Mass Flux Framework for Boundary Layer Convection. Part I: Transport. *J. Atmos. Sci.*, **66**, 1465–1487.

Nitta, T., and S. Esbensen, 1974: Heat and moisture budget analyses using BOMEX data. *Mon. Wea. Rev*, **102**, 17–28.

Nuijens, L., B. Medeiros, I. Sandu, and M. Ahlgrimm, 2014: The behavior of trade-wind cloudiness in observations and models. Part I: The major cloud components and their variability. *J. Adv. Model Earth Syst.*,.

Park, S., and C. Bretherton, 2009: The University of Washington shallow convection and moist turbulence schemes and their impact on climate simulations with the Community Atmosphere Model. *J. Climate*, **22**(12), 3449–3469.

Raymond, D. J., and Z. Fuchs, 2009: Moisture modes and the Madden-Julian oscillation. *J. Atmos. Sci.*, **22**, 3031–3046.

Rieck, M., L. Nuijens, and B. Stevens, 2012: Marine boundary-layer cloud feedbacks in a constant relative humidity atmosphere. *J. Atmos. Sci.*, **69**, 2538–2550.

Rodwell, M., and T. N. Palmer, 2007: Using numerical weather prediction to assess climate models. *Quart. J. Roy. Met. Soc.*, **133**, 129–146.

Sandu, I., A. Beljaars, T. Bechtold, P. Mauritsen, and G. Balsamo, 2012: Why is it so difficult to represent stably stratified conditions in NWP models? *J. Adv. Model Earth Syst.*, **5**, 117–133.

Sandu, I., and B. Stevens, 2011: On the factors modulating the stratocumulus to cumulus transitions. *J. Atmos. Sci.*, **68**, 1865–1881.

Sandu, I., B. Stevens, and R. Pincus, 2010: On the transitions in marine boundary layer cloudiness. **10**, 2377–2391.

Tiedtke, M., 1989: A comprehensive mass flux scheme for cumulus parametrization in large-scale models. *Mon. Wea. Rev*, **117**, 1779–1800.

Tiedtke, M., 1993: Representation of clouds in large-scale models. *Mon. Wea. Rev*, **121**(11), 3040–3061.

Tompkins, A., P. Bechtold, A. Beljaars, A. Benedetti, S. Cheinet, M. Janisková, M. Köhler, P. Lopez, and J.-J. Morcrette, 2004: Moist physical processes in the IFS: Progress and plans. ECMWF Tech. Memo. 452, 91 pp.

Tompkins, A. M., 2002: A prognostic parameterization for the subgrid-scale variability of water vapor and clouds in large-scale models and its use to diagnose cloud cover. *J. Atmos. Sci.*, **59**, 1917–1942.

von Salzen, K., N. McFarlane, and M. Lazare, 2005: The role of shallow convection in the water and energy cycles of the atmosphere. *Climate Dynamics*, **25**(7), 671–688.

Wood, R., and C. Bretherton, 2006: On the relationship between stratiform low cloud cover and lower-tropospheric stability. *J. Climate*, **19**(24), 6425–6432.